JPP Journal of Pharmacy and Pharmacology

JPP 2010, 62: 413–421

Received September 12, 2009
Accepted January 5, 2010
DOI 10.1211/jpp/62.04.0002
ISSN 0022-3573

Research Paper

Dissolution of artemisinin/polymer composite nanoparticles fabricated by evaporative precipitation of nanosuspension

Mitali Kakran[a], Nanda Gopal Sahoo[a], Lin Li[a] and Zaher Judeh[b]

[a]Schools of Mechanical and Aerospace Engineering and [b]Schools of Chemical and Biomedical Engineering, Nanyang Technological University, Singapore

Abstract

Objectives An evaporative precipitation of nanosuspension (EPN) method was used to fabricate composite particles of a poorly water-soluble antimalarial drug, artemisinin, with a hydrophilic polymer, polyethylene glycol (PEG), with the aim of enhancing the dissolution rate of artemisinin. We investigated the effect of polymer concentration on the physical, morphological and dissolution properties of the EPN-prepared artemisinin/PEG composites.

Methods The original artemisinin powder, EPN-prepared artemisinin nanoparticles and artemisinin/PEG composites were characterised by scanning electron microscopy, Fourier-transform infrared spectroscopy, differential scanning calorimetry (DSC), X-ray diffraction (XRD), dissolution testing and HPLC. The percentage dissolution efficiency, relative dissolution, time to 75% dissolution and mean dissolution time were calculated. The experimental drug dissolution data were fitted to various mathematical models (Weibull, first-order, Korsemeyer–Peppas, Hixson–Crowell cube root and Higuchi models) in order to analyse the release mechanism.

Key findings The DSC and XRD studies suggest that the crystallinity of the EPN-prepared artemisinin decreased with increasing polymer concentration. The phase-solubility studies revealed an A_L-type curve, indicating a linear increase in drug solubility with PEG concentration. The dissolution rate of the EPN-prepared artemisinin and artemisinin/PEG composites increased markedly compared with the original artemisinin powder.

Conclusions EPN can be used to prepare artemisinin nanoparticles and artemisinin/PEG composite particles that have a significantly enhanced dissolution rate. The mechanism of drug release involved diffusion and erosion.

Keywords artemisinin; crystallinity; dissolution; nanoparticles; polyethylene glycol

Introduction

Many of the drugs discovered today exhibit very poor water solubility.[1] Poorly water-soluble drugs show a number of negative clinical effects, such as high local drug concentrations at the sites of aggregate deposition, which could be associated with local toxic effects, and decreased systemic bioavailability.[2] The great challenge in pharmaceutical development is to create new formulations and efficient drug-delivery systems to overcome solubility and dissolution problems of drug candidates with poor oral bioavailability.[3] Various physical modifications can be used to enhance the solubility and dissolution rate of poorly water-soluble drugs, such as particle size reduction[4] or the development of amorphous states.[5,6] However, on a nanometer scale van der Waals forces become dominant and hence the dissolution rate may not improve as expected. These van der Waals forces cause the drug nanoparticles to agglomerate and aggregate. In order to overcome these van der Waals forces, repulsive forces should be introduced. One way to solve the problem is to adsorb hydrophilic polymers onto the particle surface to obtain steric stabilisation. Adsorbing polymers can also reduce particle size and increase surface area of the drug, which improves dissolution rates.[7] In addition, hydrophilic polymers allow more extensive wetting of drug particles, resulting in higher solubility and dissolution rates of poorly water-soluble drugs. Finally, combining a drug with an amorphous or less crystalline polymer can change the degree of crystallinity and the polymorphic form of the drug.[8] As a result, it is possible to obtain less crystalline or more amorphous drug particles with enhanced solubility and hence increased bioavailability.

Correspondence: Lin Li, School of Mechanical and Aerospace Engineering, Nanyang Technological University, 50 Nanyang Avenue, Singapore 639798.
E-mail: mlli@ntu.edu.sg

Artemisinin is a potent antimalarial drug that remains effective against the multidrug-resistant strains of *Plasmodium falciparum* malaria. It has a good intestinal permeability and can readily cross the intestinal monolayers via passive diffusion.[9] A major problem with artemisinin compounds is poor aqueous solubility,[10] resulting in poor absorption following oral administration. This poor solubility, short half-life and high first-pass metabolism may result in incomplete clearance of the parasites, resulting in recrudescence.[11]

In our previous study, nanoparticles of artemisinin were prepared using the evaporative precipitation of nanosuspension (EPN) method.[12] The drug nanoparticles exhibited approximately six times faster dissolution than the original artemisinin particles. In the present study, EPN is used to fabricate composite nanoparticles of artemisinin and polyethylene glycol (PEG) in order to further enhance the dissolution rate of artemisinin. PEG was chosen because it is water-soluble and biocompatible. Artemisinin nanoparticles and artemisinin/PEG composite nanoparticles with different ratios of artemisinin to PEG were prepared. The dissolution data for the samples were analysed statistically and fitted with various kinetic release models to examine the drug-release mechanisms.

Materials and Methods

Materials

Artemisinin was obtained from Kunming Pharmaceutical Corporation (Kunming, China). PEG 4000 was obtained from Sigma Aldrich. All reagents used were of technical grade.

Methods

Artemisinin nanoparticles and artemisinin/PEG composite particles were prepared by the EPN method. The original artemisinin powder was dissolved in ethanol (solvent) and the nanosuspension formed by quickly adding hexane (antisolvent) without the need for a surfactant or stabiliser. Drug particles in the nanosuspension were obtained by evaporation of the solvent and antisolvent under vacuum using a rotary evaporator. This was followed by overnight vacuum drying of the nanoparticles to completely evaporate all the solvents. The drug concentration in the solvent was 15 mg/ml and the solvent-to-antisolvent ratio was 1 : 20 (by volume), which was previously found to yield the smallest particle size and the highest dissolution rate.[12] The same drug concentration and solvent-to-antisolvent ratio were used to prepare the artemisinin/PEG composite particles. Artemisinin and PEG were dissolved in the common solvent (ethanol) and composite particles were formed by quickly adding the common antisolvent (hexane), followed by quick evaporation and vacuum drying. Different artemisinin-to-PEG ratios used in the composites were 1 : 1, 1 : 2 and 1 : 4 (by weight).

Characterisation

The morphology of samples was observed using a scanning electron microscope (JSM-6390LA-SEM, Jeol Co., Tokyo, Japan). The powder samples were first spread on a SEM stud and sputtered with gold. Analysis of particle size was performed using the UTHSCSA ImageTool program (Version 3.0 Dept Dental Diagnostic Science, Health Science Center, University of Texas, TX, USA; http://ddsdx.uthscsa.edu/dig/itdesc.html). Fourier-transform infrared (FTIR) spectroscopic measurements were performed using a Digilab FTS 3100 system using the KBr disk method. Differential scanning calorimetric (DSC) measurements were carried out using a PerkinElmer DSC 7 thermal analyser in the temperature range 40–250°C at a heating rate of 10°C/min in nitrogen gas. The melting point and heat of fusion were calculated using the DSC software. X-ray diffraction (XRD) was studied using theBruker AXS D8 Advance X-ray diffractometer with Cu Kα-targets at a scanning rate of 0.010 2θ/s, applying 40 kV, 40 mA, to observe the crystallinity of samples.

Dissolution studies

The in-vitro dissolution of the samples was determined using the paddle method (USP apparatus II; Verkin Dissolution Tester DIS 8000) in 900 ml distilled water. The paddle rotation was set at 200 rpm. The temperature was maintained at 37 ± 0.5°C. All the samples containing an equivalent of 360 mg artemisinin were tested for their dissolution in water. Samples of dissolved solution (1 ml) were collected after 0.5, 1, 2, 3 and 4 h' dissolution. Three dissolution tests were performed for each sample. The samples were filtered through a 0.45 μm polypropylene-reinforced Teflon membrane with polypropylene housing (Ministart-SRP 15, Saritorius, Goettingen, Germany).

For HPLC analysis, 1 ml sample was added to 200 μl 10 mol/l sodium hydroxide and the mixture heated at 45°C for 25 min and then cooled to room temperature; 150 μl glacial acetic acid was then added before injection onto the HPLC system.

HPLC was performed using an Agilent 1100 series system with ultraviolet detection[13] and a Kromasil C18 column (150 mm × 4.6 mm i.d. × 3.5 μm) (Eka Chemicals AB, Sweden). The mobile phase consisted of 75% 0.01 mol/l disodium hydrogen phosphate and 25% acetonitrile (HPLC grade) adjusted to pH 6.5 with glacial acetic acid, delivered at a flow rate of 0.8 ml/min. Detection was at 254 nm.

Phase solubility study

The phase solubility study was performed using the method reported by Higuchi and Connors.[14] Excess artemisinin was added into the PEG solutions of various concentrations in screw-capped vials. The concentrations of PEG used were 0, 2, 4, 6, 8 and 10 mmol/l. The vials were shaken continuously in a thermostatically controlled water bath at 24, 37 and 52°C for 72 h until equilibrium was achieved (this duration was previously shown to be sufficient to reach equilibrium). Once equilibrium was reached, a 1 ml sample of each solution was filtered through a 0.45 μm polypropylene-reinforced Teflon membrane and diluted with water before HPLC analysis.

The stability constant (K_s) at the three different temperatures (i.e. 24, 37 and 52°C) was calculated from the linear section of the phase solubility diagrams from equation 1:

$$K_s = \frac{slope}{S_0(1-slope)} \quad (1)$$

where S_0 is the intrinsic solubility of artemisinin in the absence of PEG, and the slope refers to the gradient of artemisinin solubility (mmo/l) plotted against PEG concentration (mmol/l).[15]

The enthalpy change (ΔH) for the artemisinin/PEG binary system was investigated using the temperature-dependent characteristic of the stability constant based on the van't Hoff equation:[16]

$$\ln K_s = -\frac{\Delta H}{RT} + \frac{\Delta S}{R} \tag{2}$$

where T is the absolute temperature (Kelvin), R is the gas constant (8.314 J/mol per K), and ΔS is the entropy change; ΔH was calculated from the slope of the plot of $\ln K_s$ against $1/T$, after least square linear regression analysis.

The Gibbs free energy of transfer (ΔG) of artemisinin from pure water to the aqueous solution of PEG at each temperature was calculated using equation 3:[17]

$$\Delta G = -RT \ln K_s \tag{3}$$

Statistical analysis and mathematical modelling of release kinetics

The percent dissolution efficiency (%DE) for each formulation was calculated as the percent ratio of area under the dissolution curve up to the time t, to that of the area of the rectangle described by 100% dissolution at the same time:[18]

$$\%\,DE = \left(\frac{\int_0^t y.dt}{y_{100}.t} \right) 100 \tag{4}$$

The time for 75% of the drug to dissolve ($t_{75\%}$) was calculated using SigmaPlot software (SigmaPlot 2001 Version 7, Systat Software Inc., Chicago, IL, USA). The mean dissolution time (MDT) was calculated using equation 5:[19]

$$MDT = \frac{\sum_{i=1}^{n} t_{mid} \Delta M}{\sum_{i=1}^{n} \Delta M} \tag{5}$$

where i is the dissolution sample number, n is the number of dissolution times, t_{mid} is the time at the midpoint between times t_i and t_{i-1}, and ΔM is the amount of artemisinin (μg) dissolved between times t_i and t_{i-1}.

A multiple comparison test was used to determine the significance of differences between the various samples by means of the non-parametric Kruskal–Wallis H-test using ranks. The Kruskal–Wallis statistic (H) was calculated using equation 6 in order to accept or reject the null hypothesis that there is no significant difference between the amounts of various samples dissolved during the dissolution test:[20]

$$H = \frac{12}{N(N+1)} \times \left[\frac{(\Sigma R_a)^2}{n_a} + \frac{(\Sigma R_b)^2}{n_b} + \frac{(\Sigma R_c)^2}{n_c} + \frac{(\Sigma R_d)^2}{n_d} + \frac{(\Sigma R_e)^2}{n_e} + \frac{(\Sigma R_f)^2}{n_f} \right] - 3(N+1) \tag{6}$$

where $\sum R_a$, $\sum R_b$, $\sum R_c$, $\sum R_d$, $\sum R_e$ and $\sum R_f$ are the sums of ranks for the original artemisinin, artemisinin/PEG physical mixture (1 : 1), EPN-prepared artemisinin and EPN-artemisinin/PEG ratios 1 : 1, 1 : 2 and 1 : 4, respectively, n_a, n_b, n_c, n_d, n_e and n_f denote the respective number of dissolution tests done for each sample (which is 3 in all cases) and N is the total number of dissolution tests performed for all the samples, which is equal to 18 ($N = 6 \times 3$).

Individual differences between the samples were then evaluated using a post-hoc Nemenyi's test for equal sample sizes. Mean significant difference (MSD) between rank means was calculated using equation 7:

$$\text{MSD} = q \times \text{SE} \tag{7}$$

where q is the value obtained from the q distribution table using number of samples involved ($k = 6$) and degrees of freedom of infinity for $\alpha = 0.05$. SE is the standard error calculated using equation 8:

$$SE = \sqrt{\frac{k(N+1)}{12}} \tag{8}$$

where k is the number of samples (6 in our case). The value of MSD calculated was then compared with the absolute differences between pairs of rank means. If the absolute difference was greater than MSD, the difference between the two samples was significant.[20]

In-vitro drug release data were fitted to various kinetic release models[19,21,22] using equations 9–13:

First order:

$$\ln\left(1 - \frac{M_t}{M_\infty}\right) = k_1 t \tag{9}$$

Korsemeyer–Peppas:

$$\frac{M_t}{M_\infty} = k' t^n \tag{10}$$

Weibull:

$$\frac{M_t}{M_\infty} = 1 - \exp(-k_s.t^n) \tag{11}$$

Higuchi:

$$M_t = K\sqrt{t} \tag{12}$$

Hixson–Crowell cube root:

$$(M_\infty)^{1/3} - (M_\infty - M_t)^{1/3} = k_{1/3}t \qquad (13)$$

where M_t and M_∞ correspond to the amount of drug dissolved at a particular time t and at infinite time, respectively. Various other terms viz. k_1, k', k_s, K and $k_{1/3}$ refer to the release kinetic constants obtained from the first-order, Korsemeyer–Peppas, Weibull, Higuchi and Hixson–Crowell cube root models, respectively. Model fitting using equations 9–13 was accomplished using the Sigma plot software.

Results

Particle morphology

From Figure 1 it can be seen that the diameters of the EPN-prepared artemisinin particles were in the range 100–360 nm, with needle-like morphology. Particles of the original artemisinin powder lacked uniformity in size and were larger (5–50 μm) than those prepared by the EPN method. The EPN-prepared artemisinin showed more uniform nanoparticles. The particles of PEG and artemisinin/PEG physical mixture were very large compared with the EPN-prepared artemisinin/PEG composite particles (450–950 nm). As shown in Figure 1, the artemisinin particles in artemisinin/PEG composites were coated individually with PEG. Different artemisinin : PEG ratios gave similar and individually coated drug particles.

FTIR study

The FTIR spectrum of the original artemisinin powder (Figure 2) showed absorption peaks at 1736 cm^{-1} (stretching vibrations of C=O due to the lactone) and at 832, 883 and 1117 cm^{-1} due to the peroxide. The EPN-prepared artemisinin showed a similar spectrum, indicating that the chemical structure of artemisinin was not changed during the EPN process. The spectrum of PEG showed a broad band at 3450 cm^{-1}, which was attributed to the presence of -OH stretching. Another important band observed at 1105 cm^{-1} was due to the presence of C–O stretching. Comparison of the

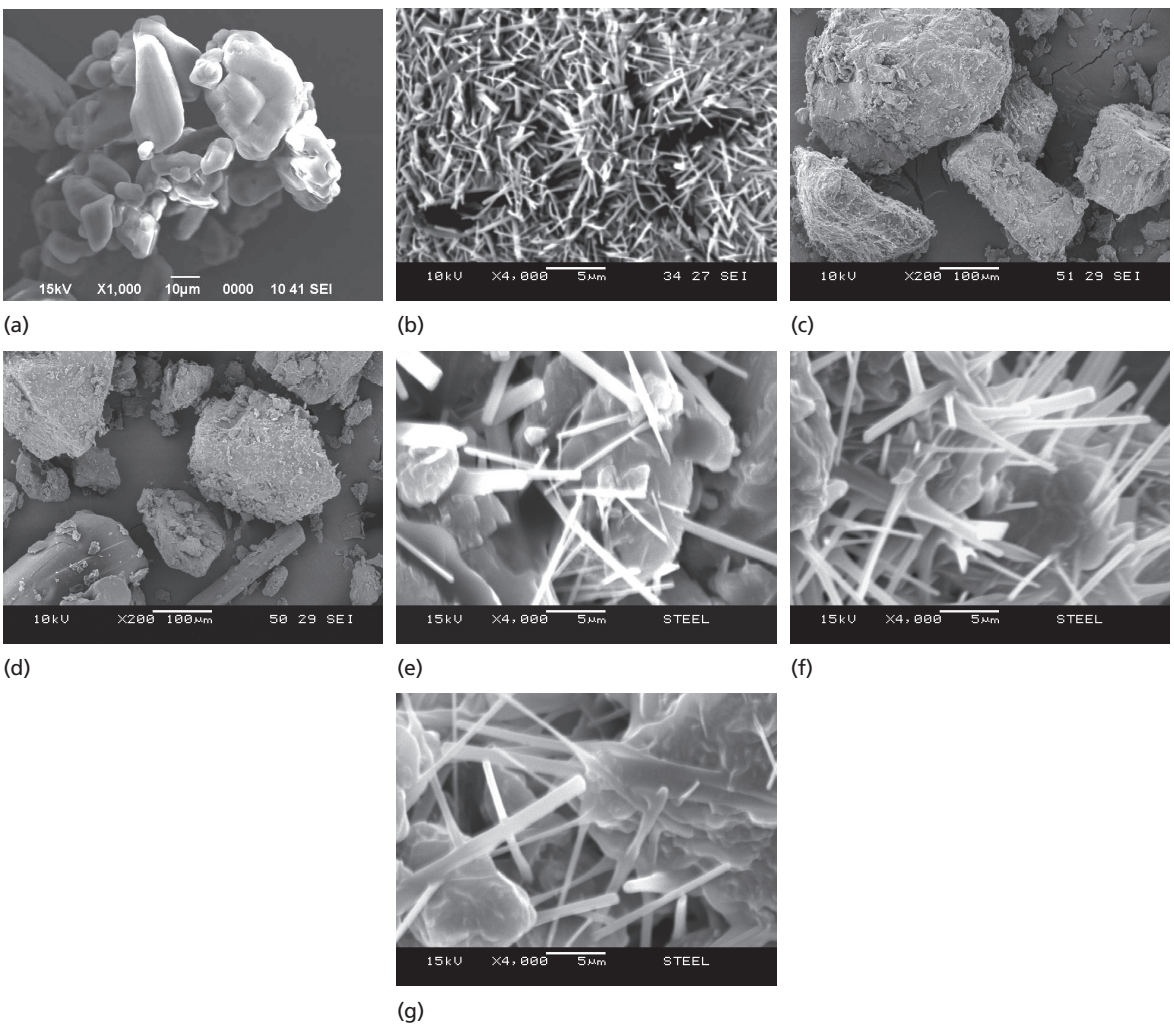

Figure 1 Scanning electron microphotographs of (a) original artemisinin powder, (b) EPN-prepared artemisinin nanoparticles, (c) PEG, (d) artemisinin/PEG physical mixture, and EPN-prepared artemisinin/PEG composites with different ratios: (e) 1 : 1, (f) 1 : 2 and (g) 1 : 4

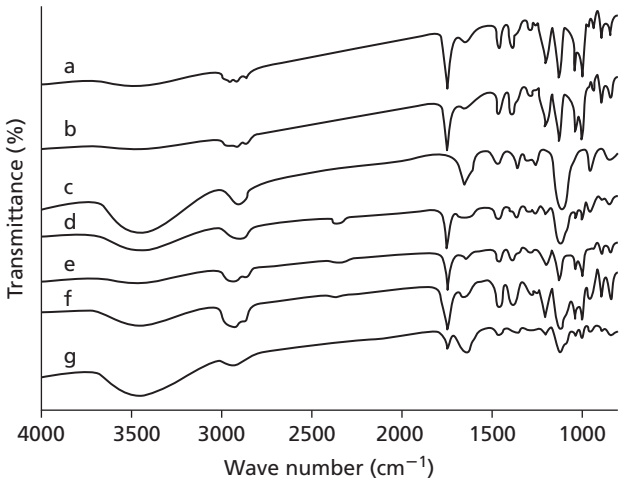

Figure 2 Fourier-transform infrared spectra of (a) original artemisinin powder, (b) EPN-prepared artemisinin, (c) PEG, (d) artemisinin/PEG physical mixture (1 : 1) and EPN-prepared artemisinin/PEG composites with different ratios: (e) 1 : 1, (f) 1 : 2 and (g) 1 : 4

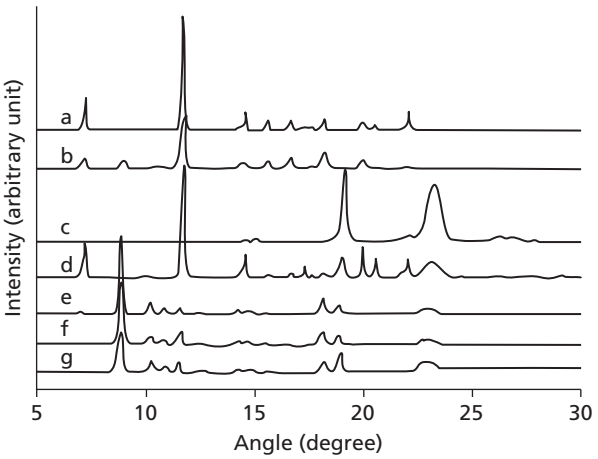

Figure 3 X-ray diffractogram of (a) original artemisinin powder, (b) EPN-prepared artemisinin, (c) PEG, (d) artemisinin/PEG physical mixture (1 : 1) and EPN-prepared artemisinin/PEG composites with different ratios: (e) 1 : 1, (f) 1 : 2 and (g) 1 : 4

spectra of the EPN-prepared artemisinin/PEG composites showed no differences in the position of the absorption peak. The absence of shifts in the wave numbers of the FTIR peaks for the EPN-prepared artemisinin/PEG composites and the physical mixture indicated a lack of significant interaction between artemisinin and PEG in the EPN-prepared composites.

Drug crystallinity

The XRD patterns of the artemisinin powder in Figure 3 displayed numerous distinct peaks at 2θ of 7.29°, 11.78°, 14.65°, 15.63°, 16.64°, 18.23°, 20.0° and 22.1°, which suggested that the drug was in a crystalline form. The diffraction spectrum of PEG showed two prominent peaks with the highest intensity at 2θ of 19.2° and 23.3°. The EPN-prepared artemisinin showed a similar diffraction pattern but with a lower peak intensity, suggesting that the crystallinity of artemisinin decreased during the EPN process. A new diffraction peak appeared at $2\theta = 9.24°$ for the EPN-prepared artemisinin, implying that there was a slight change in the crystal structure. For the artemisinin/PEG physical mixtures, all the peaks from artemisinin were present with slightly lower intensity, and no new peaks were observed, suggesting the absence of interaction between the drug and PEG in the physical mixture. For the EPN-prepared artemisinin/PEG composites, new diffraction peaks appeared at 2θ = 9.22°, 10.24° and 10.79° but with lower peak intensity, suggesting that the crystallinity of artemisinin/PEG composites decreased during the EPN process. The new peaks observed suggest some physical interaction between the drug and PEG, which led to the change in crystal structure. The FTIR results showed that there was no chemical interaction between artemisinin and PEG, but the XRD data suggest that the addition of PEG introduced some changes in the crystal structure of artemisinin. From the XRD data we can conclude that the EPN process led to a change in only the crystal structure of the artemisinin and artemisinin/PEG composites. The crystalline nature of the drug was still maintained, but the relative reduction of diffraction intensity of artemisinin in the EPN-prepared composite suggests that the crystallinity of the drug was reduced.

DSC was used to understand the effect of the EPN process on the thermal properties of artemisinin. It can be seen from Figure 4 that the original artemisinin powder used in this study had a sharp melting endothermic peak at 156°C. The DSC scan of PEG showed a single sharp endotherm at 59°C due to the melting of PEG. The endothermic melting peak of the EPN-prepared artemisinin was shifted slightly to a lower temperature. For the EPN-prepared artemisinin/PEG composites, the artemisinin endothermic peak was at a lower temperature than that of the original artemisinin powder, the EPN-prepared artemisinin and the corresponding physical mixture, indicative of a certain loss of crystallinity. The heat of fusion of the

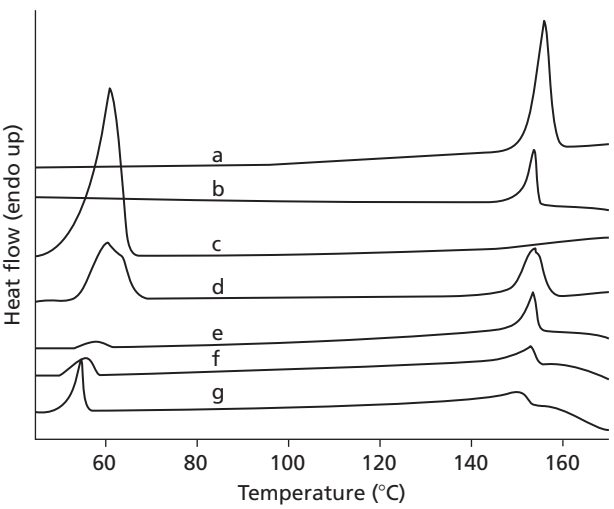

Figure 4 Thermogram of (a) original artemisinin powder, (b) EPN-prepared artemisinin, (c) PEG (d) artemisinin/PEG physical mixture (1 : 1) and EPN-prepared artemisinin/PEG composites with different ratios: (e) 1 : 1, (f) 1 : 2 and (g) 1 : 4

Table 1 Dissolution characteristics of the original artemisinin powder, EPN-prepared artemisinin and artemisinin/PEG composites and artemisinin/PEG physical mixture (1 : 1)

Sample	T_m	ΔH_f (J/g)	$t_{75\%}$ (h)	$RD_{0-5\ h}$	$\%DE_{4\ h}$	$MDT_{4\ h}$ (h)
Original artemisinin	156.0	76.20	>4	1	9.29	1.16
EPN artemisinin	154.0	59.18	3.86	4.17	49.89	1.10
Artemisinin/ PEG mixture (1 : 1)	155.7	59.68	>4	1.27	11.84	1.11
EPN-prepared artemisinin/PEG						
1 : 1	153.3	55.55	1.74	6.59	69.77	1.06
1 : 2	152.6	54.26	1.14	8.70	76.79	0.86
1 : 4	150.0	51.31	0.86	11.22	82.23	0.71

$T_{m,}$ melting temperature; ΔH_f, heat of fusion; $t_{75\%}$, time for 75% dissolution; RD, relative dissolution: %DE, percent dissolution efficiency; MDT, mean dissolution time.

original artemisinin powder was higher than that of the EPN-prepared artemisinin. From Table 1, it can be clearly seen that the heat of fusion of the EPN-prepared artemisinin/PEG composites decreased with increasing polymer concentration. The heat of fusion of the EPN-prepared artemisinin/PEG composites was lower than their corresponding physical mixture (Figure 4, Table 1). Since heat of fusion is proportional to the crystallinity in the samples, these results suggest that the crystallinity of the artemisinin particles decreased when they were dispersed in the EPN-prepared composites, which is also supported by the XRD results.

Phase solubility study

The phase-solubility profiles of artemisinin in the presence of PEG are shown in Figure 5. The phase solubility of artemisinin increased linearly with increasing PEG concentration and temperature. The linear solubility curves could be classified as type A_L, suggesting that the system was first order.[14] The linear relationship also suggested that dilution of an artemisinin/PEG solution during administration into the body would not cause precipitation of artemisinin, regardless of the extent of dilution. The solubility was increased approximately 9-fold at the highest polymer concentration at 24°C, and a similar tendency was observed at 37°C and 52°C. Similar results have been reported for several other drugs using water-soluble carriers, which were attributed to the formation of weakly soluble complexes[23,24] and/or the cosolvent effect of the carrier.[25]

The thermodynamic parameters (ΔG, ΔH and K_s) for the system are shown in Table 2. The correlation coefficient (r^2) of the van't Hoff plot was 0.9963, indicating a very good fit. An indication of the transfer process of artemisinin from pure water to an aqueous solution of PEG was obtained from the values of Gibbs free energy change, which here provides information about whether or not the reaction is favourable for solubilisation of the drug in the aqueous carrier solution. The negative ΔG values at different temperatures indicate spontaneous solubilisation of artemisinin. The negative enthalpy (ΔH) indicate that the reaction was exothermic, which favoured the formation of the artemisinin/PEG composite. The stability constant (K_s) decreased with increasing temperature, which may be due to a decrease in interaction forces (i.e. van der Waals and hydrophobic forces).[26]

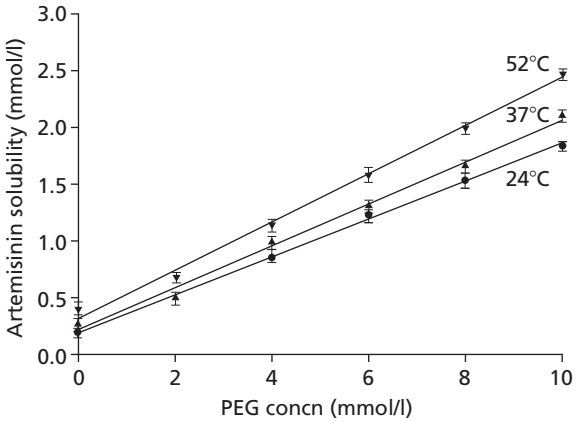

Figure 5 Phase solubility diagram of PEG/artemisinin binary system at different temperatures

Table 2 Stability constants (K_s) and thermodynamic parameters for the solubilisation of artemisinin in aqueous solutions of PEG at different temperatures

Temperature (°C)	K_s (M^{-1})	ΔG (kJ/mol)	ΔH (kJ/mol)
24	1002.40	−17.06	−11.65
37	804.79	−17.24	
52	667.36	−17.57	

ΔG, Gibbs free energy of transfer; ΔH, enthalpy change.

Dissolution study

It is evident from Figure 6 that the dissolution of the original artemisinin was very low (13.1%) whereas the EPN-prepared artemisinin showed enhanced dissolution (75.9%) within 4 h. The dissolution of artemisinin from the physical mixture (16.4%) was similar to that of artemisinin powder. The dissolution of artemisinin from all the EPN-prepared artemisinin/PEG composites was markedly increased compared with the original artemisinin and EPN-prepared artemisinin. The dissolution of artemisinin increased with increasing amount of drug carrier in the EPN-prepared artemisinin/PEG composites. The greatest improvement (100%) was observed at the highest carrier level (i.e. artemisinin : PEG = 1 : 4).

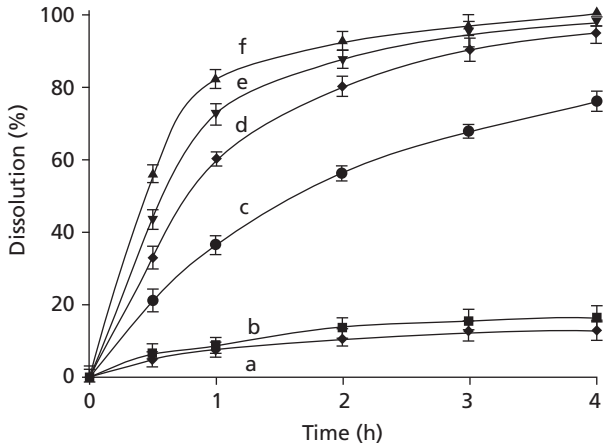

Figure 6 Dissolution profiles of (a) original artemisinin powder, (b) EPN-prepared artemisinin, (c) PEG, (d) artemisinin/PEG physical mixture (1 : 1) and EPN-prepared artemisinin/PEG composites with different ratios: (e) 1 : 1, (f) 1 : 2 and (g) 1 : 4

It can be seen from Table 1 that the original artemisinin and the artemisinin/PEG physical mixture (1 : 1) did not reach even 75% dissolution within 4 h. The EPN-prepared artemisinin reached 75% dissolution in 3.86 hours, whereas the EPN-prepared artemisinin/PEG composites showed shorter 75% dissolution times, confirming that the dissolution of artemisinin is influenced by PEG. The MDT values calculated for all the samples investigated (Table 1) also support this finding. MDT reflects the time for the drug to dissolve and is the first statistical moment for the cumulative dissolution process that provides an accurate release rate of a drug.[27] A higher MDT value indicates a greater retardation of drug release.[28] The MDT value for the original artemisinin was very high (1.16 h). This value was decreased in EPN-prepared artemisinin. For the EPN-prepared artemisinin/PEG composites, the MDT values decreased drastically with increasing PEG concentration. The lowest MDT (0.710 h) was observed for the 1 : 4 artemisinin/PEG composite. From Table 1 it an be seen that the values of RD_{0-5h} and $\%DE_{4h}$ (1.27 and 11.84, respectively) for the physical mixture of artemisinin and PEG (1 : 1) were lower than those of the EPN-prepared artemisinin/PEG composite at the same ratio (6.59 and 69.77, respectively), indicating that the EPN-prepared artemisinin/PEG composites had better dissolution than the corresponding physical mixture. The RD_{4h} and RD_{0-5h} values revealed that the greatest improvement in dissolution was with the highest concentration of PEG in the EPN-prepared artemisinin/PEG composites (1 : 4 ratio).

Discussion

The value of Kruskal–Wallis statistic (H) was 15.83 ($H_{calculated}$; $H_{critical}$ = 11.07). As $H_{calculated} > H_{critical}$, the null hypothesis was rejected in favour of the alternative hypothesis, indicating significant differences between the different samples ($P < 0.05$). There was an overall significant difference in the amounts of various samples dissolved after 4 h during the dissolution test (H = 15.83, $P < 0.05$). Using Nemenyi's multiple comparison test, it was concluded that during the dissolution test the 1 : 4 ratio artemisinin/PEG composites had significantly more drug dissolved than the original drug and the artemisinin/PEG physical mixture ($P < 0.05$).

According to the Noyes–Whitney equation, the saturation solubility and dissolution rate of a drug can be increased by reducing the particle size in order to increase the surface area.[29] The particle size of the original artemisinin powder was reduced to 100–360 nm for artemisinin nanoparticles and 450–950 nm in the composites prepared by the EPN method, which increased the dissolution of the EPN-prepared artemisinin and artemisinin/PEG composites.

The DSC and XRD studies showed that the crystallinity of artemisinin in the EPN-prepared artemisinin nanoparticles and artemisinin/PEG composite particles was lower than that of the original artemisinin powder, particularly in the case of the 1 : 4 ratio artemisinin/PEG composite. The extent of crystallinity also influences the dissolution of the drug: an amorphous or metastable form will dissolve more quickly than crystalline materials because of higher internal energy and greater molecular motion.[5,6] From the results and analysis, we conclude that the EPN-prepared artemisinin and artemisinin/PEG composite nanoparticles showed faster rate and higher extent of dissolution than the original artemisinin powder. An increased dissolution rate could be translated into improved bioavailability following oral administration.

To understand the mechanism of drug release, the dissolution profiles of artemisinin were fitted to various kinetic release models, summarised in Table 3. The best fit for the EPN prepared artemisinin/PEG composites ranked in the order of Weibull = first-order > Korsemeyer–Peppas = Higuchi > Hixson–Crowell.

Since the Weibull model exhibited excellent fitting of the experimental data, it can be used to analyse the drug release kinetics. The n values obtained were smaller than 1 for all the samples, which implied that the dissolution curve had a parabolic shape with a higher initial slope followed by an exponential decline.[21] Table 3 shows that the release constant k_s was less than 1 for the EPN-prepared artemisinin and mostly greater than 1 for the EPN-prepared artemisinin/PEG composites. In both cases, the k_s values were greater than that of the original artemisinin, which implies that dissolution was faster with the EPN-prepared artemisinin and artemisinin/PEG composites.

The first-order release kinetics also fitted the experimental data perfectly. In first-order kinetics, the release of drug is proportional to the amount of drug remaining in the nanoparticle interior; the amount of drug released per unit of time therefore diminishes over time. The first-order release constant (k_1) was much higher for the EPN-prepared artemisinin and artemisinin/PEG composites than for the original artemisinin powder, indicating increased dissolution rate.

The analysis of experimental data using the Korsemeyer–Peppas equation, as well as the interpretation of the corresponding release exponent values (n), led to a better understanding of the balance between purely diffusional and purely erosion-controlled mechanisms. The values of

Table 3 Statistical parameters obtained after fitting drug release data to various release kinetic models

Model		Original artemisinin	EPN artemisinin	EPN artemisinin/PEG		
				1 : 1	1 : 2	1 : 4
First order	k_1 (h^{-1})	0.0428	0.3975	0.8356	1.1740	1.6400
	r^2	0.7501	0.9902	0.9970	0.9960	0.9968
Korsemeyer–Peppas	k' (h^{-n})	0.0735	0.3585	0.5532	0.6558	0.7495
	n	0.4393	0.5631	0.4262	0.3247	0.2355
	r^2	0.9955	0.9932	0.9780	0.9745	0.9807
Weibull	k_s (h^{-n})	0.0764	0.4459	0.8439	1.1650	1.5780
	n	0.4624	0.8502	0.9520	0.9281	0.8842
	r^2	0.9959	0.9993	0.9975	0.9966	0.9976
Higuchi	K ($mg/h^{1/2}$)	6.9440	38.0600	51.6500	55.8600	59.0700
	r^2	0.9904	0.9888	0.9702	0.9213	0.8397
Hixson–Crowell	$k_{1/3}$ ($mg^{1/3}/h$)	0.0645	0.5136	1.0610	1.4690	1.6690
	r^2	0.7387	0.9676	0.9810	0.9817	0.9578

diffusional exponent n (obtained from the slopes of the fitted Korsemeyer–Peppas model) ranged from 0.2355 to 0.4393. From these values we could conclude that all the samples tended to exhibit Fickian diffusional characteristics, as the corresponding values of n were lower than the standard value for Fickian release behaviour (i.e. 0.45).[30] Only the EPN-prepared artemisinin showed an n value marginally above 0.45, indicating weak non-Fickian release behaviour.

The Higuchi model also showed a very good fit, the values for the first-order constant of dissolution k increasing for the EPN-prepared artemisinin and artemisinin/PEG composites (maximum for ratio 1 : 4) compared with that for the original artemisinin powder. A similar fit was shown by the Hixson–Crowell cube root law, which describes the release from systems where there is a change in surface area and diameter of particles. It follows an erosion release mechanism. Similar to other kinetic release models, the value of the Hixson–Crowell release constant $k_{1/3}$ was higher for the artemisinin/PEG composites and EPN-prepared artemisinin than the original artemisinin. These results support diffusional mechanistic phenomena as well as the erosion release mechanism.

Conclusions

This study has demonstrated that EPN can be used to prepare artemisinin nanoparticles and artemisinin/PEG composite particles with significantly enhanced dissolution rates. The crystallinity of the drug decreased with increasing PEG concentration, which improved the dissolution of artemisinin particles. The release of artemisinin from the composite particles followed both the diffusional and erosion release mechanisms, as demonstrated by the excellent fits of the drug release data to the Korsemeyer–Peppas, Higuchi, Hixson–Crowell cube root and first order kinetic models. The artemisinin nanoparticles and artemisinin/PEG composite particles produced using this method have good potential for improved drug delivery in much smaller doses than with commercial preparation methods.

Declarations

Conflict of interest

The Author(s) declare(s) that they have no conflicts of interest to disclose.

Funding

The authors acknowledge financial support from Lee Kuan Yew Postdoctoral Fellowship, Nanyang Technological University, Singapore.

References

1. Lipinski CA *et al*. Experimental and computational approaches to estimate solubility and permeability in drug discovery and development settings. *Adv Drug Deliv Rev* 2001; 6: 3–26.
2. Yalkowsky SH. *Techniques of Solubilization of Drugs.* New York: Marcel Dekker, 1981.
3. Lipinski C. Poor aqueous solubility – an industry wide problem in drug delivery. *Am Pharm Rev* 2002; 5: 82–85.
4. Subramaniam B *et al*. Pharmaceutical processing with supercritical carbon dioxide. *J Pharm Sci* 1997; 86: 885–890.
5. Hancock BC, Zografi G. Characteristics and significance of the amorphous state in pharmaceutical systems. *J Pharm Sci* 1997; 86: 1–12.
6. Grau MJ *et al*. Nanosuspensions of poorly soluble drugs: reproducibility of small scale production. *Int J Pharm* 2000; 196: 155–157.
7. Patel R, Patel M. Preparation, characterization, and dissolution behavior of a solid dispersion of simvastatin with polyethylene glycol 4000 and polyvinylpyrrolidone k30. *J Dispersion Sci Tech* 2008; 29: 193–204.
8. Duncan QM, Craig. The mechanisms of drug release from solid dispersions in water-soluble polymers. *Int J Pharm* 2002; 231: 131–144.
9. Augustijns P *et al*. Transport of artemisinin and sodium arsenate in Caco-2 intestinal epithelial cells. *J Pharm Sci* 1996; 85: 577–579.
10. Barradell LB, Fitton A. Artesunate: a review of its pharmacology and therapeutic efficacy in the treatment of malaria. *Drugs* 1995; 50: 714–741.
11. Titulaer HAC *et al*. Formulation and pharmacokinetics of arthemisinin and its derivatives. *Int J Pharm* 1991; 69: 83–92.

12. Kakran M *et al*. Fabrication of drug nanoparticles by evaporative precipitation of nanosuspension. *Int J Pharm* 2010; 383: 285–292.
13. Zhao SS. High-performance liquid chromatographic determination of artemisinin (qinghaosu) in human plasma and saliva. *Analyst* 1987; 112: 661–664.
14. Higuchi T, Connors KA. Phase solubility techniques. *Adv Anal Chem Instr* 1965; 4: 117–212.
15. Wong JW, Yuen KH. Inclusion complexation of artemisinin with α-, β-, and γ-cyclodextrins. *Drug Dev Ind Pharm* 2003; 29: 1035–1044.
16. Van Etten RL *et al*. Acceleration of phenyl cleavage by cycloamyloses. A model of enzymatic specificity. *J Am Chem Soc* 1967; 89: 3242–3252.
17. Simonelli AP *et al*. Dissolution rates of high energy sulfathiazole povidone coprecipitation II. Characterization of form of drug controlling its dissolution rate via solubility studies. *J Pharm Sci* 1976; 65: 355–361.
18. Khan KA. The concept of dissolution efficiency. *J Pharm Pharmacol* 1975; 27: 48–49.
19. Costa FO *et al*. Comparison of dissolution profiles of ibuprofen pellets. *J Control Release* 2003; 89: 199–212.
20. Jones DS. *Pharmaceutical Statistics.* London: Pharmaceutical Press, 2002.
21. Costa P, Lobo JMS. Modeling and comparison of dissolution profiles. *Eur J Pharm Sci* 2001; 13: 123–133.
22. Labastie M *et al*. Tablet dissolution parameters: a statistical evaluation. *J Pharm Biomed Anal* 1992; 10: 1105–1108.
23. Cirri M *et al*. Characterization of ibuproxam binary and ternary dispersions with hydrophilic carriers. *Drug Dev Ind Pharm* 2004; 30: 65–74.
24. Sekikawa H *et al*. Inhibitory effects of polyvinylpyrrolidone on the crystallization of drugs. *Chem Pharm Bull* 1978; 26: 118–126.
25. Chiou WL. Pharmaceutical applications of solid dispersions systems: X-ray diffraction and aqueous solubility studies on griseofulvine-polyethylene glycol 6000 systems. *J Pharm Sci* 1977; 66: 989–991.
26. Ashwinkumar CJ, Moji CA. Hygroscopicity, phase solubility and dissolution of various substituted solfobutylether-β-cyclodextrins (SBE) and danazol-SBE inclusion complexes. *Int J Pharm* 2001; 212: 177–186.
27. Reppas C, Nicolaides E. Analysis of drug dissolution data. In: Dressman JB, Lennernas H (eds), *Oral Drug Absorption: Prediction And Assessment (Drugs and the Pharmaceutical Sciences).* New York: Marcel Dekker, 2000: 229–254.
28. Vueba ML *et al*. Influence of cellulose ether polymers on ketoprofen release from hydrophilic matrix tablets. *Eur J Pharm Biopharm* 2004; 58: 51–59.
29. Noyes AA, Whitney WR *et al*. The rate of solution of solid substances in their own solutions. *J Am Chem Soc* 1987; 19: 930–934.
30. Korsemeyer RW *et al*. Mechanisms of solute release from porous hydrophilic polymers. *Int J Pharm* 1983; 15: 25–35.